Check for updates

Histopathology

Histopathology 2024, **84**, 776–793. DOI: 10.1111/his.15121

Spindle cell rhabdomyosarcomas: With *TFCP2* rearrangements, and novel *EWSR1::ZBTB41* and *PLOD2::RBM6* gene fusions. A study of five cases and review of the literature

Martina Bradová,[1,2] Elaheh Mosaieby,[1,2] Michael Michal,[1,2] Tomáš Vaněček,[2] Stanislav Kormunda Ing,[3] Petr Grossmann,[2] Olena Koshyk,[4] Zdeněk Kinkor,[1,2] Šimon Laciok,[5] Antónia Nemcová,[6] Ľubomír Straka,[7] Mihaela Farkas,[8] Michal Michal[1,2] & Marián Švajdler[1,2,9]

[1]*Department of Pathology, Faculty of Medicine in Plzen, Charles University, Prague,* [2]*Bioptic Laboratory Ltd, Plzen,* [3]*Division of Information Technologies and Statistics, Faculty of Medicine in Pilsen, Charles University, Pilsen, Czech Republic,* [4]*Medical Laboratory CSD, Kyiv, Ukraine,* [5]*Department of Pathology, Třinec Hospital, Třinec, Czech Republic,* [6]*Medicyt Ltd, Košice,* [7]*Unilabs, Diagnostic Pathology Centre, Prešov, Slovakia,* [8]*Onco Team Diagnostic, București, Romania and* [9]*Cytopathos, Ltd, Bratislava, Slovakia*

Date of submission 19 September 2023
Accepted for publication 2 December 2023

Bradová M, Mosaieby E, Michal M, Vaněček T, Ing S K, Grossmann P, Koshyk O, Kinkor Z, Laciok Š, Nemcová A, Straka Ľubomí, Farkas M, Michal M & Švajdler M (2024) *Histopathology* **84**, 776–793. https://doi.org/10.1111/his.15121

Spindle cell rhabdomyosarcomas: With *TFCP2* rearrangements, and novel *EWSR1::ZBTB41* and *PLOD2::RBM6* gene fusions. A study of five cases and review of the literature

Aims: Spindle-cell/sclerosing rhabdomyosarcomas (SS-RMS) are clinically and genetically heterogeneous. They include three well-defined molecular subtypes, of which those with *EWSR1/FUS::TFCP2* rearrangements were described only recently. This study aimed to evaluate five new cases of SS-RMS and to perform a clinicopathological and statistical analysis of all *TFCP2*-rearranged SS-RMS described in the English literature to more comprehensively characterize this rare tumour type.

Methods and Results: Cases were retrospectively selected and studied by immunohistochemistry, fluorescence *in situ* hybridization with *EWSR1/FUS* and *TFCP2* break-apart probes, next-generation sequencing (Archer FusionPlex Sarcoma kit and TruSight RNA Pan-Cancer Panel). The PubMed database was searched for relevant peer-reviewed English reports. Five cases of SS-RMS were found. Three cases were *TFCP2* rearranged SS-RMS, having *FUSex6::TFCP2ex2* gene fusion in two cases and triple gene fusion *EWSR1ex5::TFCP2ex2*, *VAX2ex2::ALKex2* and *VAX2intron2::ALKex2* in one case. Two cases showed rhabdomyoblastic differentiation and spindle-round cell/sclerosing morphology, but were characterized by novel genetic fusions including *EWSR1ex8::ZBTB41ex7* and *PLOD2ex8::RBM6ex7*, respectively. In the statistical analysis of all published cases, *CDKN2A* or *ALK* alterations, the use of standard chemotherapy and age at presentation in the range of 18–24 years were negatively correlated to overall survival.

Conclusion: *EWSR1/FUS::TFCP2*-rearranged SS-RMS is a rare rhabdomyosarcoma subtype, affecting

Address for correspondence: M Bradová, Sikl's Department of Pathology, Faculty of Medicine in Pilsen, Charles University, E. Benese 13, Pilsen 305 99, Czech Republic. e-mail: bradova@biopticka.cz

Abbreviations: FISH, fluorescencein situ hybridization; HPFs, high powerfields; IHC, immunohistochemistry; OS, overallsurvival; PD-L2, PDCD1LG2; RMW, Rhabdomyosarcomas; SMA, smooth muscle actin; SS-RMS, spindle-cell/sclerosingrhabdomyosarcomas; TRKi, tyrosinkinase inhibitors.

© 2023 John Wiley & Sons Ltd.

predominantly young adults with average age at presentation 34 years (median 29.5 years; age range 7–86 years), with a predilection for craniofacial bones, rapid clinical course with frequent bone and lung metastases, and poor prognosis (3-year overall survival rate 28%).

Keywords: *ALK*, *CDKN2A/B*, epithelioid, *EWSR1*, *FUS*, intraosseous, molecular genetics, MyoD1, *PLOD2*, *RBM6*, rhabdomyosarcoma, spindle cell, *TFCP2*, *ZBTB41*

Introduction

Rhabdomyosarcomas (RMS) are malignant tumours with rhabdomyoblastic differentiation represented by a spectrum of cell phenotypes. Immunohistochemistry (IHC) using the myogenic nuclear regulatory proteins MyoD1 (MYF3) and myogenin (MYF4) with variable desmin expression across RMS subtypes is essential to achieve a diagnosis of RMS.[1] Most recently, PAX7 has been described as a sensitive IHC marker for skeletal muscle differentiation.[2]

RMS are divided into four basic types according to the latest 5th edition of the WHO classification of soft tissue and bone tumours,[3] which includes embryonal RMS, alveolar RMS, pleomorphic RMS, and spindle cell/sclerosing RMS (SS-RMS).[4]

SS-RMS was first described as a histological subtype of embryonal RMS, but since the 2013 the WHO classification of soft tissue and bone tumours, they have been classified separately.[5,6] Over the years, it became obvious that SS-RMS is genetically and clinically very heterogeneous. As of today, three well-defined molecular subtypes are recognized, including (i) congenital spindle cell RMS with *VGLL2/NCOA1/NCOA2 or CITED2* gene rearrangements,[7,8] (ii) *MYOD1*-mutant spindle cell/sclerosing RMS,[9–12] and (iii) spindle cell RMS with *TFCP2* rearrangements.[13–15] However, very recent studies have reported additional potential molecular subtypes, including cases with both *NCOA3* as well as *VGLL3* rearrangements.[16–18] A subset of SS-RMS usually harbouring *EWSR1/FUS*::*TFCP2* or *MEIS1*::*NCOA1/2* gene fusions shows a strong predilection for primary bone involvement.[19]

EWSR1/FUS::TFCP2 rearranged SS-RMS were first described by Watson *et al.*[13] They show spindle to epithelioid morphology, tend to affect craniofacial bones, especially the jaws of young adults, and are often associated with a rapid clinical course, resistance to adjuvant treatment, and poor prognosis.

In this study we aimed to analyse five cases of SS-RMS using targeted DNA and RNA sequencing. In addition, we collected and statistically analysed clinicopathological and molecular genetic data of all *TFCP2*-rearranged SS-RMS cases described in the English literature to better characterize this rare entity.

Materials and Methods

CASE SELECTION

The study followed the rules set by the Faculty Hospital in Pilsen Ethics Committee. Informed consent was not required. Five cases of SS-RMS were identified in the files of the authors and their clinicopathological features were reviewed and recorded. Architecture, tumour cell shape (spindle, epithelioid, round), stromal features, the presence of necrosis, and bone invasion were evaluated, and the mitotic index was determined by counting a total field size of 2.4 mm^2 (approximately equivalent to 10 high-power fields [HPFs; ×400]). The clinical follow-up information was obtained from the treating clinicians and from the referring pathologists.

HISTOLOGY AND IHC

For conventional microscopy, tissues were fixed in formalin, routinely processed, embedded in paraffin, cut, and stained with haematoxylin & eosin.

For IHC, 4-μm-thick sections were cut from paraffin blocks and mounted on positively charged slides (TOMO, Matsunami Glass IND, Osaka, Japan). Sections were processed on a BenchMark ULTRA (Ventana Medical Systems, Tucson, AZ, USA), deparaffinized, and subjected to heat-induced epitope retrieval by immersion in a CC1 solution (pH 8.6) at 95°C. The primary antibodies used in this study are summarized in Table 1. Visualization was performed using the ultraView Universal DAB Detection Kit (Roche, Tucson, AZ, USA) and ultraView Universal Alkaline Phosphatase Red Detection Kit (Roche). The slides were counterstained with Mayer's haematoxylin. Appropriate positive controls were employed.

MOLECULAR GENETIC STUDY

Archer FusionPlex assay

In cases 1–4, the in-house customized version of ArcherDX FusionPlex Sarcoma kit (Boulder, CO, USA)

13652559, 2024, 5, Downloaded from https://onlinelibrary.wiley.com/doi/10.1111/his.15121 by Ukraine - Cochrane, Wiley Online Library on [17/12/2024]. See the Terms and Conditions (https://onlinelibrary.wiley.com/terms-and-conditions) on Wiley Online Library for rules of use; OA articles are governed by the applicable Creative Commons License

Table 1. Antibodies used for immunohistochemical study

Antibody specificity	Clone	Dilution	Antigen retrieval/time	Source
AE1/AE3	AE1/AE3 + PCK26	RTU	EnVision High pH/30 min	Ventana
OSCAR	IsoType:IgG2a	1:100	EnVision High pH/30 min	Covance
EMA	E29	1:400	EnVision High pH/30 min	Dako
ALK	ALK-01	RTU	CC1/64	Ventana
Desmin	D33	1:200	EnVision High pH/30 min	Dako
Myogenin	F5D	RTU	CC1/52	Ventana
MyoD1	EP212	RTU	CC2/68	Ventana
PAX7	Monoclonal	1:500	CC2/56	Ventana
Caldesmon	h-CD	RTU	FLEX High pH/ 30 min	Dako
SMA	1A4	1:500	EnVision High pH/30 min	Dako
S-100 protein	Polyclonal	RTU	EnVision High pH/30 min	Dako
SOX 10	SP267	RTU	CC1/64 min	Cell Marque
CD34	QBEnd/10	1:100	CC1/64 min	Dako
CD31	JC70A	1:40	EnVision High pH/30 min	Dako
ERG	EPR3864	RTU	CC1/52 min	Ventana
SATB2	CL0276	1:100	CC1/52 min	Ventana
SS18-SSX	E9X9V	1:2000	CC1/52 min	Cell Signaling

CC1, EDTA buffer pH 8.6 at 95°C; CC2, Citrate buffer pH 6.0 at 92°C; EnVision High pH 9.0 at 97°C; EnVision Low pH 6.0 at 97°C; min, minutes; RTU, Ready to use.

was used to construct a cDNA library for detecting fusion transcripts and point mutations in 88 and 14 genes, respectively (File S1). All steps were performed according to the manufacturer's instructions, and the library was sequenced on an Illumina platform as described previously.[20]

Illumina TruSight oncology 500 and TruSight RNA Pan-Cancer panel assays

Case 5 was analysed using the TruSight Oncology 500 assay from Illumina (San Diego, CA, USA). This panel analyses both DNA and RNA. The DNA analysis interrogates 523 genes for single nucleotide variants (SNVs) and indels. However, for the RNA analysis the original set of probes for fusion detection (which interrogates only 55 genes) was replaced with TruSight RNA Pan-Cancer Panel (Illumina) targeting 1385 genes. The complete list of genes in both the DNA and RNA part of the analysis can be found on the manufacturer's website.[21,22] Data analysis for fusion detection was performed using Dragen RNA app v. 4.0.4 (Illumina). The analysis was otherwise performed as reported previously.[23]

DETECTION OF *EWSR1* AND *ZBTB41* REARRANGEMENTS BY FLUORESCENCE *IN SITU* HYBRIDIZATION

The dual-colour, commercial break-apart probe EWSR1 Break Apart fluorescence *in situ* hybridization (FISH) Probe Kit (Vysis/Abbott Molecular Diagnostics, Des Plaines, IL, USA), was used in this interphase FISH assay to detect the presence of an *EWSR1* gene region (22q12) rearrangement. For the confirmation of the *ZBTB41* gene (1q31.3) rearrangement in case 4, custom-designed break-apart probe SureFish ZBTB41 Break Apart probe (Agilent Technologies, Santa Clara, CA, USA) was used.

The detailed procedure and interpretation were performed in the same way as previously described by our group.[24]

13652559, 2024, 5, Downloaded from https://onlinelibrary.wiley.com/doi/10.1111/his.15121 by Ukraine - Cochrane, Wiley Online Library on [17/12/2024]. See the Terms and Conditions (https://onlinelibrary.wiley.com/terms-and-conditions) on Wiley Online Library for rules of use; OA articles are governed by the applicable Creative Commons License

REVIEW OF THE LITERATURE

The PubMed database was searched for relevant peer-reviewed reports published in English, using a combination of the following keywords: "sclerosing rhabdomyosarcoma", "spindle cell rhabdomyosarcoma", "*TFCP2*", "*EWSR1::TFCP2*", and/or "*FUS::TFCP2*". From over 800 articles published in the period from 1962 to July 2023, we selected all relevant studies dealing with SS-RMS with a *TFCP2* rearrangement. Twenty-three articles were identified and the clinical information, IHC results, and genetic data were extracted and analysed together with our data from cases 1 to 3 that harboured *TFCP2* fusions (File S2).

STATISTICAL ANALYSIS

Statistical analysis was performed using SW SAS (Cary, NC, USA). The descriptive statistics such as absolute and relative frequencies, mean, standard deviation, variance, median, interquartile range, minimum, and maximum were calculated. The Kaplan–Meier analyses was used to calculate the overall survival (OS). The Gehan Wilcoxon test, log-rank test, and Cox regression hazard model including hazard ratio calculations were used to assess the clinical impact of the examined covariates. Statistical significance was determined at the level of 5%. The cases with *EWSR1::ZBTB41* (case 4) and *PLOD2::RBM6* (case 5) gene fusions were excluded from statistical analyses.

Results

Clinical data, selected morphological features, and IHC and molecular genetic results are summarized in Tables 2 and 3.

Case 1 was a 51-year-old woman who was admitted to the hospital with a diagnosis of periprosthetic hyperplastic gingivitis of the maxilla without any clinical suspicion of malignancy. The patient underwent biopsy with a diagnosis of malignant epithelial tumour most compatible with sarcomatoid squamous cell carcinoma and was incompletely resected without adjuvant treatment. Four years later, the tumour recurred, and the patient underwent maxillectomy. The tumour was 55 mm in size and was composed of short fascicles of epithelioid to spindle-shaped cells with small eosinophilic nucleoli and irregular nuclear borders (Figure 1A,B). No rhabdomyoblasts were present. Tumour cells were surrounded by myxocollagenous stroma. There were 5 mitoses/10 HPF;

Table 2. Clinical data, morphological features, type of therapy, and follow-up information

Case no.	Age/ sex	Site	Symptoms	Size mm	Morphology	Stroma	Mitoses/ 10HPF	Necrosis	Therapy	CHT/ RT	Biological therapy	Metastasis	Follow-up (months)
1	51/F	Maxilla	Hyperplastic gingivitis	55	Epithelioid/ spindle cell	Collagenous, myxoid	5	Absent	Resection	No	No	No	48 AWD
2	7/F	Mandible	Pain in mandible	59	Epithelioid/ spindle cell	Focally myxoid	15	Absent	None	CHT, RT	Yes	No	8 AWD
3	65/M	Supraumbilical area soft tissues	None	95	Spindle cell/ hypocellular	Collagenous, loose myxoid, lymphoid follicles	16	Present	Resection	No	No	No	38 ANED
4	48/F	Retroperitoneum	Pain in sacral region	NA	Small round blue cell tumour	Not present	17	Absent	None—inoperable	CHT	No	Liver, spleen, bones, retroperitoneum	19 DOD
5	15/F	Femur	None	NA	Epithelioid spindle cell	Collagenous/ sclerotic	15	Present	NA	NA	NA	NA	1 LOF

ANED, Alive not evidence of disease; AWD, Alive with disease; CHT, Chemotherapy; DOD, Died of disease; F, Female; LOF, Lost to follow-up; NA, Not available; M, Male; RT, Radiotherapy.

13652559, 2024, 5, Downloaded from https://onlinelibrary.wiley.com/doi/10.1111/his.15121 by Ukraine - Cochrane, Wiley Online Library on [17/12/2024]. See the Terms and Conditions (https://onlinelibrary.wiley.com/terms-and-conditions) on Wiley Online Library for rules of use; OA articles are governed by the applicable Creative Commons License

Table 3. Immunohistochemical results and molecular genetic data of our five cases

No	AE1/3/ OSCAR	EMA	ALK	Desmin	Myogenin	MyoD1	PAX7	Caldesmon	SMA	S100	SOX10	CD34	CD31	ERG	SATB2	SSX/SS18	Molecular genetic
1	Diffuse moderate to weak	N	Diffuse cytoplasmic	N	N	Diffusely	N	N	N	N	N	N	NA	N	Few cells	N	*FUSex6::TFCP2ex2*
2	Focally +	N	Diffuse cytoplasmic / perinuclear	Few cells	N	Diffusely	N	N	N	Focally +	N	N	NA	N	Focally +	N	*EWSR1ex5::TFCP2ex2, VAX2ex2::ALKex2, VAX2intron2::ALKex2*
3	Focally +	Few cells	Diffuse cytoplasmic	N	Few cells	Diffusely	N	Diffusely	Focally +	N	N	N	NA	N	N	N	*FUSex6::TFCP2ex2*
4	N	N	Focally + weak	Diffusely	Diffusely	Diffusely	N	N	N	N	N	Weakly positive	NA	N	N	N	*EWSR1ex8::ZBTB41ex7*
5	N	N	N	Diffusely	Focally +	Diffusely	N	N	Diffusely	N	N	N	N	N	Diffusely	Focally +/ N	*PLOD2ex8::RBM6ex7*
																	PTPRT c.795C > A p.(Tyr265Ter)
																	PDGFRA amplification

+, Positive; N, –Negative; SMA, Smooth muscle actin.

necrosis was absent. Immunohistochemically, the tumour cells were diffusely positive for cytokeratin cocktail AE1/AE3 (Figure 1C) and OSCAR as well as for MyoD1 (Figure 1D). Myogenin, desmin, PAX7, smooth muscle actin (SMA), and h-caldesmon were negative, along with endothelial and neurogenic markers. ALK showed strong cytoplasmic expression (Figure 1E). RNA-sequencing revealed *FUSex6::TFCP2ex2* gene fusion. The patient was alive with disease 48 months after diagnosis.

Case 2 was a 7-year-old girl diagnosed with mandibular pain of suspected inflammatory origin and was treated by physiotherapy. A subsequent computed tomography (CT) scan revealed a lytic lesion in the anterior mandible measuring 32 mm in the largest diameter with soft-tissue involvement of maximal size 38 mm. The patient underwent a biopsy with a diagnosis of sarcoma and received two cycles of chemotherapy (vincristine, dactinomycin, ifosfamide and vincristine, doxorubicin, ifosfamide). There was no therapeutic effect and the soft-tissue component kept growing, eventually reaching 60 mm. The tumour consisted of a variable cellular proliferation of epithelioid to spindle-shaped cells that were organized in vague fascicles with intervening myxoid to collagenous stroma (Figure 2A,B). The nuclear membrane was irregular, with large eosinophilic nucleoli. No rhabdomyoblastic differentiation was noted. The mitotic count was 15 mitoses/10 HPF; necrosis was absent. Tumour cells were focally immunopositive for AE1/AE3 (Figure 2C) and OSCAR. MyoD1 showed diffuse nuclear expression (Figure 2D), desmin was only focally positive, and myogenin, PAX7, SMA, and h-caldesmon were completely negative. Additionally, S100 protein (Figure 2E) and SATB2 were focally positive. ALK showed diffuse but weak cytoplasmic and perinuclear expression (Figure 2F).

RNA-sequencing detected three gene fusions, including in-frame *EWSR1ex5::TFCP2ex2*, out-of-frame *VAX2ex2::ALKex2*, and unknown frame status fusion with intron exonisation *VAX2intron2::ALKex2* (Figure 3A,B).

The patient was alive with disease 8 months after diagnosis and recently received radiotherapy and two cycles of chemotherapy (topotecan and carboplatin) followed by two cycles of irinotecan combined with crizotinib. The size of the tumour decreased by 37% and the patient was scheduled for surgery.

Case 3 was a 65-year-old man with a 9.5-cm large tumour in the supraumbilical soft tissues with skin ulceration. The lesion was resected with an unknown margin status. The referring diagnoses included superficial myxofibrosarcoma, synovial sarcoma, or

13652559, 2024, 5, Downloaded from https://onlinelibrary.wiley.com/doi/10.1111/his.15121 by Ukraine - Cochrane, Wiley Online Library on [17/12/2024]. See the Terms and Conditions (https://onlinelibrary.wiley.com/terms-and-conditions) on Wiley Online Library for rules of use; OA articles are governed by the applicable Creative Commons License

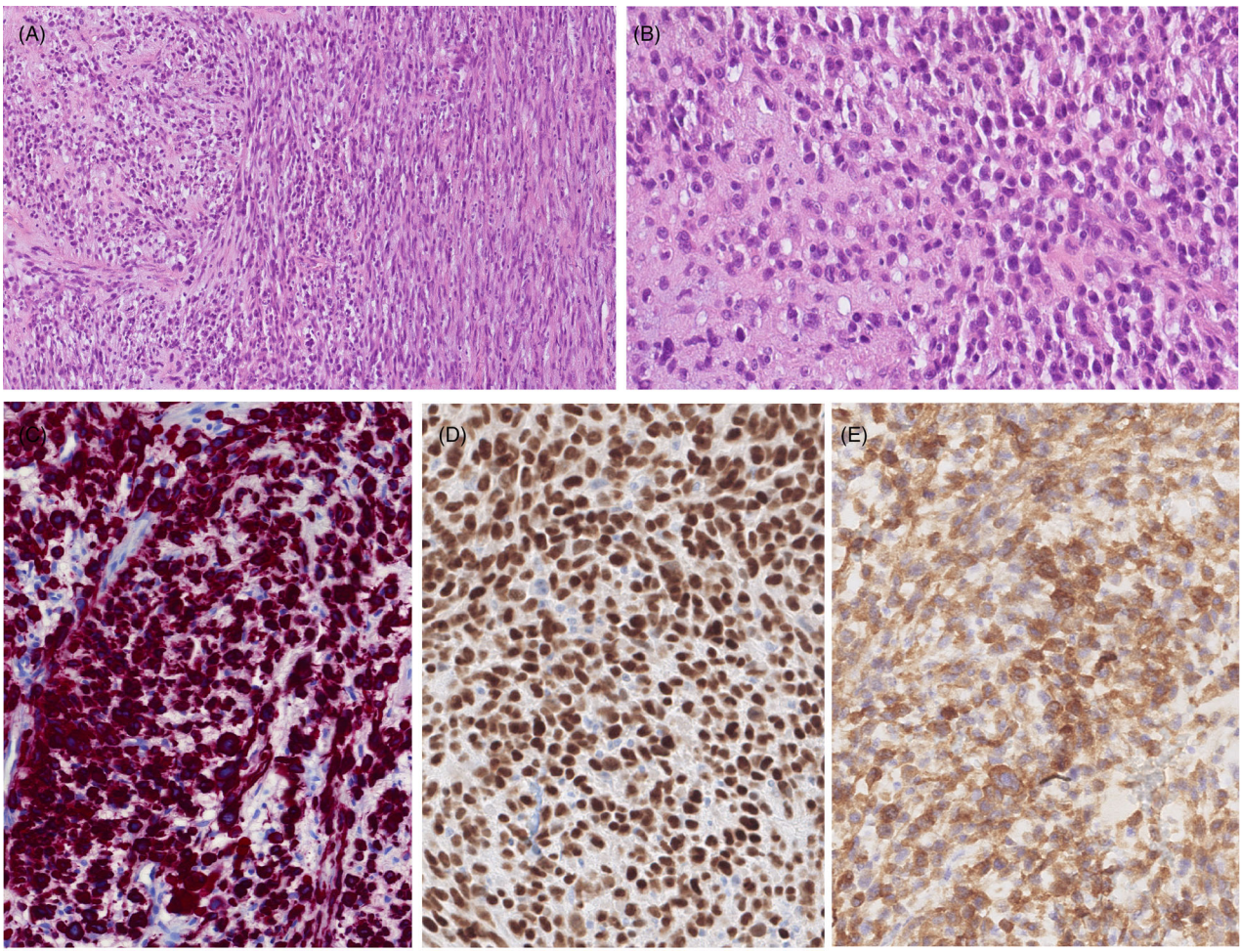


Figure 1. The tumour was composed of short fascicles of spindle-shaped (**A**) to epithelioid (**B**) cells with small eosinophilic nucleoli and irregular nuclear borders. Stroma was collagenous/sclerotic (**B**) and occasionally myxoid. Tumour cells were diffusely positive for *AE1*/3 (**C**) and *MyoD1* (**D**). *ALK* showed cytoplasmic immunoexpression (**E**).

high-grade leiomyosarcoma. The tumour consisted of variably cellular fascicles of spindle cells (Figure 4A), which gradually transformed into areas with haphazardly arranged epithelioid cells; no rhabdomyoblasts were present (Figure 4B). The stroma was mostly collagenous but occasionally myxoid, with few lymphoid aggregates mainly at the tumour periphery. Mitotic activity reached 16 mitoses/10 HPF, small areas of necrosis, and perineurial invasion were present. Immunohistochemically, pan-cytokeratins (AE1/AE3, OSCAR) (Figure 4C), EMA, SMA, and desmin were focally positive. MyoD1 (Figure 4D) and h-caldesmon (Figure 4E) were diffusely positive (the latter predominantly in spindle cell areas), whereas myogenin and PAX7 were negative. ALK showed diffuse cytoplasmic expression (Figure 4F). Next-generation sequencing (NGS) was performed and *FUSex6::TFCP2ex2* gene fusion was found. The patient was alive without evidence of disease 38 months after diagnosis.

Case 4 was 48-year-old-woman investigated for sacral pain, which was found to be caused by a retroperitoneal tumour with massive metastatic spread in the retroperitoneum, bones, liver, and spleen. A biopsy was performed and the tumour was diagnosed as Ewing sarcoma. Since the tumour was inoperable, the patient was treated by chemotherapy (vincristine, ifosfamide, doxorubicin, and etoposide) in a modified regimen due to bicytopenia. Tumour progressed with multiple bone metastases, of which one focus in the acromioclavicular joint was resected. It was composed of solid sheets of small round-to-ovoid cells with only occasional loose myxoid stromal areas (Figure 5A). No rhabdomyoblastic differentiation was noted. There were 17 mitoses/10 HPF; necrosis was absent.

13652559, 2024, 5, Downloaded from https://onlinelibrary.wiley.com/doi/10.1111/his.15121 by Ukraine - Cochrane, Wiley Online Library on [17/12/2024]. See the Terms and Conditions (https://onlinelibrary.wiley.com/terms-and-conditions) on Wiley Online Library for rules of use; OA articles are governed by the applicable Creative Commons License

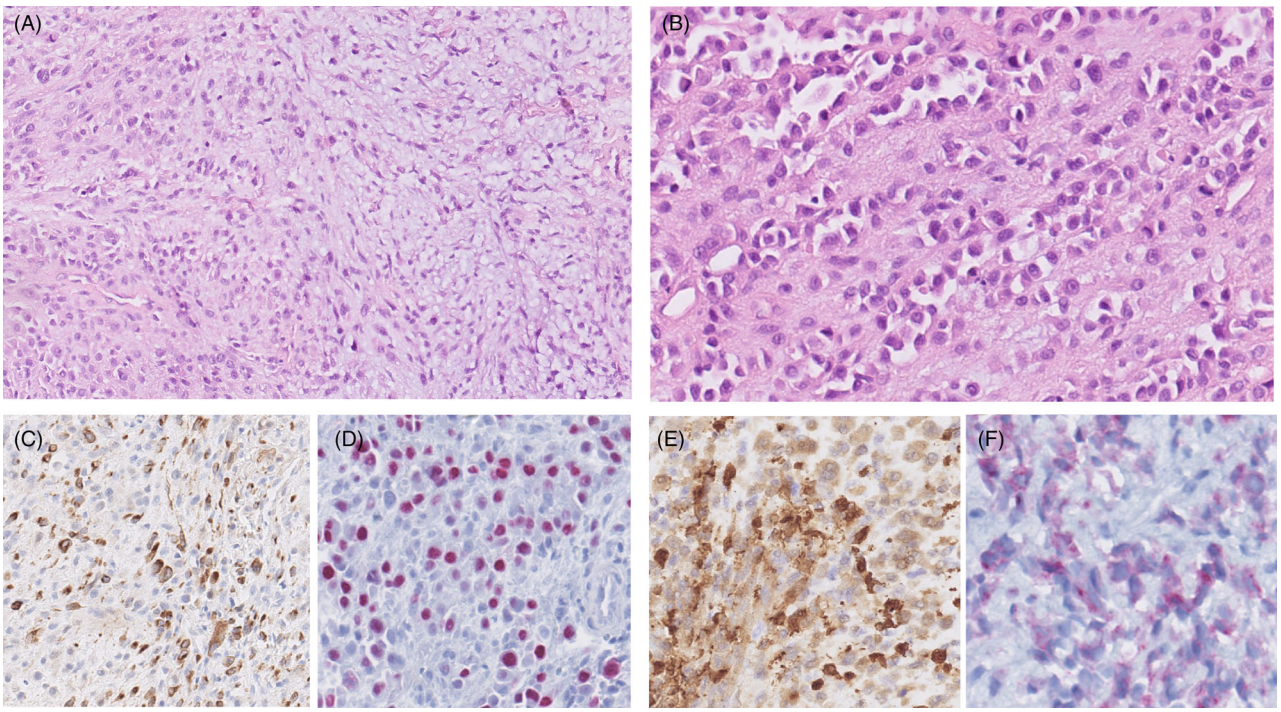


Figure 2. Case 2 was rather bland-looking, with a vague fascicular architecture (**A**) and was composed of spindle-shaped to epithelioid or rhabdoid tumour cells occasionally with areas reminiscent of alveolar spaces (**B**). Tumour cells showed irregular expression of *AE1/3* (**C**), *MyoD1* (**D**), *S100* protein (**E**), and *ALK* (**F**).

Desmin, myogenin, and MyoD1 were diffusely positive and ALK showed focal cytoplasmic expression (Figure 5B–E). Tumour cells were negative for pan-cytokeratins (AE1/3 and OSCAR), CD99, and NKX2.2. An in-frame *EWSR1ex8::ZBTB41ex7* fusion was detected, which, to our best knowledge, has not been previously reported (Figure 6A) This novel fusion was further confirmed by FISH using both *EWSR1* and *ZBTB41* probes (Figure 6B). A scanned whole slide image of the case is available at https://pathpresenter.net/public/display?token=d40feb2e.

Nineteen months later, the patient died due to tumour progression and concurrent bone marrow depletion caused by extensive tumour infiltration and drug-induced pancytopenia, associated with the development of sepsis and pulmonary thromboembolic disease.

Case 5 was 15-year-old female who had a pathological fracture of the distal femur due to an underlying neoplastic process. The tumour consisted of variably cellular proliferation of epithelioid, plasmacytoid-to-spindle-shaped cells with high nuclear pleomorphism, irregular chromatin, and small nucleoli that were embedded in a fibrosclerotic stroma. There were large necrotic areas and the mitotic count reached up to 15 mitoses/10 HPF. While there was a surprising aberrant SATB2 expression, no osteoid formation was noted (Figure 7A,B). Tumour cells were focally positive for desmin, MyoD1, and myogenin and diffuse expression of SMA was noted (Figure 7C–E), whereas pan-cytokeratins and ALK were negative. DNA and RNA sequencing revealed *PTPRT* c.795C>A p.(Tyr265Ter) gene mutation (with allelic frequency 19%) and low-level *PDGFRA* amplification. In addition, in-frame gene fusion between exon 8 of the *PLOD2* gene and exon 7 of the *RBM6* gene (Figure 7F) was detected as well. A scanned whole-slide image of the case is available at https://pathpresenter.net/public/display?token=e398c6c1.

The patient was referred to the children's orthopaedic oncology centre, but was lost to further follow-up.

REVIEW OF THE LITERATURE

Twenty-three articles reporting 66 cases of *TFCP2*-rearranged SS-RMS (our three cases included) were found in the English literature.[13–15,19,25–40] There were 39 female and 25 male patients (the gender was unknown in two cases). The average age at

13652559, 2024, 5, Downloaded from https://onlinelibrary.wiley.com/doi/10.1111/his.15121 by Ukraine - Cochrane, Wiley Online Library on [17/12/2024]. See the Terms and Conditions (https://onlinelibrary.wiley.com/terms-and-conditions) on Wiley Online Library for rules of use; OA articles are governed by the applicable Creative Commons License

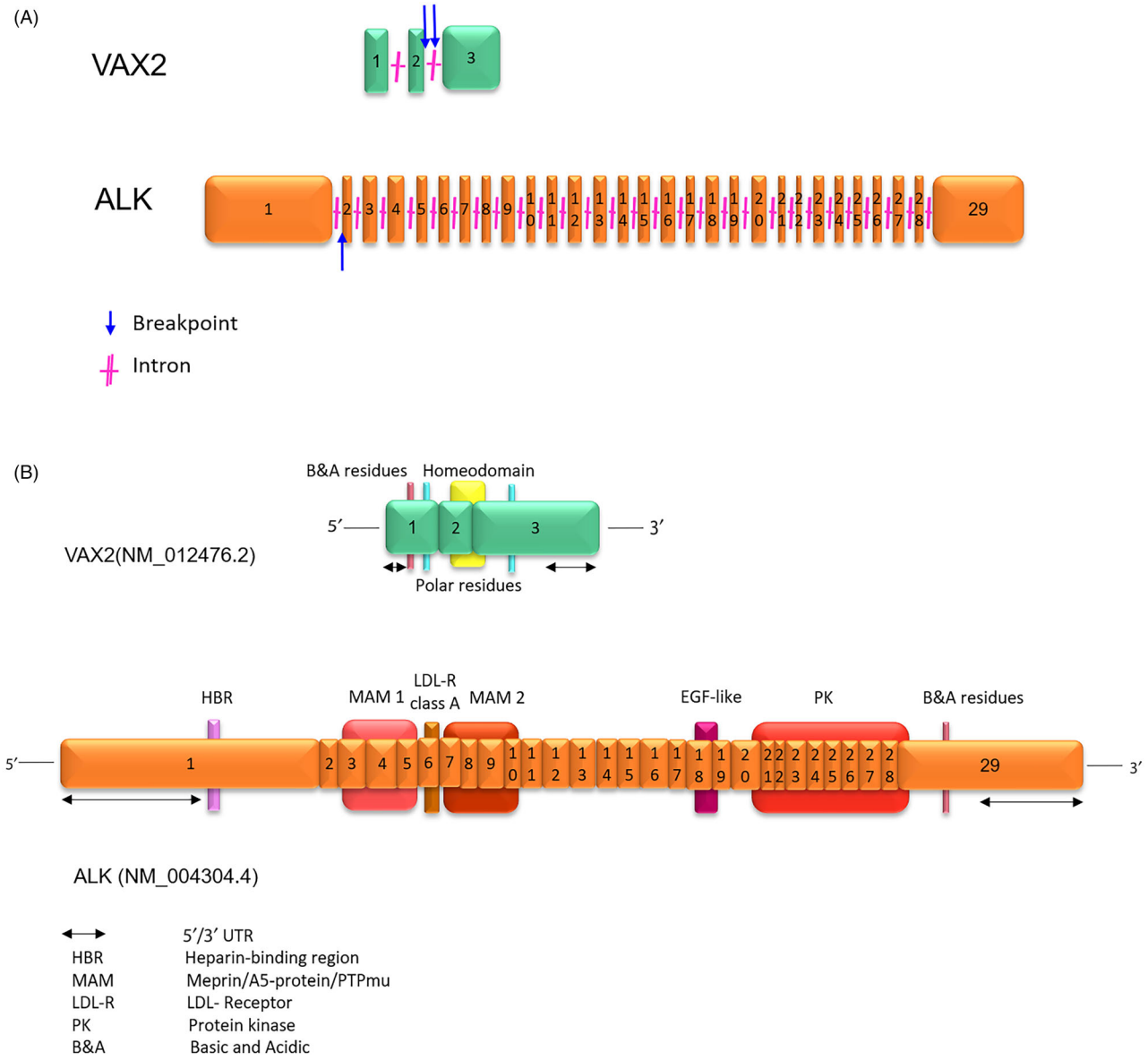


Figure 3. Case 2 was characterized by triple gene fusion involving the genes *VAX2* and *ALK*. (**A**) The structure of the genes with indicated breakpoints. The fusion takes place at the end of exon 2 of *VAX2* and within its intron and *ALK* contributes to the fusion with a breakpoint before exon 2. (**B**) Displays transcripts of these two genes, as well as their specific domains. [Colour figure can be viewed at wileyonlinelibrary.com]

presentation was 34 years (median 29.5 years; age range 7–86 years). Forty-four cases (~72%) were localized in the head and neck (H&N) region, including craniofacial bones, with 29 cases presenting in the mandible (n = 15) or maxilla (n = 14). Other locations comprised pelvic bones (n = 8), other bones of the axial skeleton (n = 6), peritoneum and abdominal wall (n = 2), femur (n = 1), chest wall and shoulder (n = 2), and the urinary bladder (n = 1). Two cases were of unknown locations. The average tumour size was 59 mm.

The tumours were composed of admixture of different cell phenotypes including spindle, epithelioid, and round cells. The pure spindle phenotype was present in 12 cases, pure epithelioid phenotype in six cases, and pure round cell phenotype in one case. The combination of spindle- and epitheloid-morphology was the most common and appeared in 38 cases (including one case with giant cells). One case showed a mixture of round- and spindle-cell morphology and one case showed a combination of all three cell types. Rhabdomyoblasts were exceptional; they were present

13652559, 2024, 5, Downloaded from https://onlinelibrary.wiley.com/doi/10.1111/his.15121 by Ukraine - Cochrane, Wiley Online Library on [17/12/2024]. See the Terms and Conditions (https://onlinelibrary.wiley.com/terms-and-conditions) on Wiley Online Library for rules of use; OA articles are governed by the applicable Creative Commons License

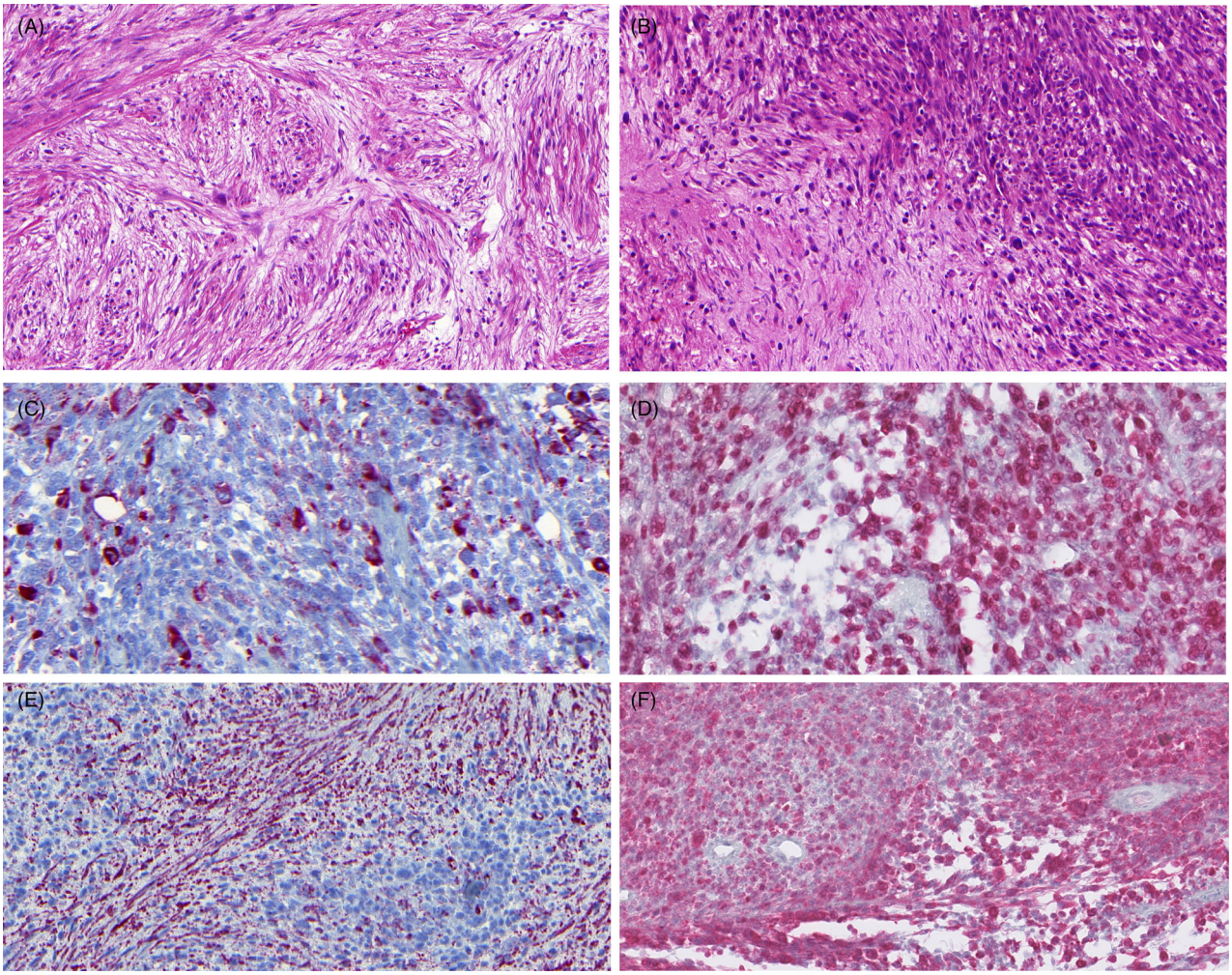


Figure 4. Tumour in case 3 was composed of closely intermingled hypo- and hypercellular areas, the former being composed of short whirling fascicles of elongated spindle-shaped cells (**A**). In contrast, the hypercellular areas consisted of haphazardly arranged epithelioid/rhabdoid tumour cells with higher nuclear pleomorphism and mitotic activity (**B**). Tumour cells were focally positive for *AE1/3* (**C**) and diffusely positive for *MyoD1* (**D**). H-caldesmon predominantly decorated the spindle cells (**E**). *ALK* showed diffuse cytoplasmic expression (**F**). [Colour figure can be viewed at wileyonlinelibrary.com]

focally in only seven cases and always admixed with dominant epithelioid- and spindle-cell phenotypes.

By IHC, SS-RMS cases were positive for MyoD1 (58/60 of cases, 96.7%), desmin (59/64, 92.2%), ALK (52/60, 86.7%), myogenin (47/62, 75.8%), and for pan-cytokeratins (31/49, 63.2%). Smooth-muscle markers tested in a subset of cases were also sometimes positive, with SMA positivity detected in 9/18 cases (50%) and h-caldesmon expression present in 2/17 cases (11.8%). PAX7 was not generally investigated across the previously reported cases, but all our cases were negative (n = 3).

Molecular genetic testing was performed in all included cases, with *FUS::TFCP2* gene fusion being confirmed in 40 cases (60.6%), including double gene fusion *FUS::TFCP2* and *TIMP3::ALK* in one case[39] and a triple gene fusion *FUS::TFCP2* combined with *VAX2ex2::ALKex2* and *VAX2intron2::ALKex2* gene fusions in another case. *EWSR1::TFCP2* gene fusion was present in 21 cases (31.8%). *TFCP2*-rearrangement without a known partner was detected by FISH in two cases (3.0%) and *FUS*-rearrangement without a partner was found in three cases (4.5%).

Deletion of the *ALK* gene was found in 11 cases and two cases carried *ALK* gene amplification by RNA sequencing.[13–15,41]

Thirteen cases harboured homozygous deletion of *CDKN2A/B*,[14,15,36,38–40] including one case with chromothripsis of 1p and 3p chromosomes[14] and one

13652559, 2024, 5, Downloaded from https://onlinelibrary.wiley.com/doi/10.1111/his.15121 by Ukraine - Cochrane, Wiley Online Library on [17/12/2024]. See the Terms and Conditions (https://onlinelibrary.wiley.com/terms-and-conditions) on Wiley Online Library for rules of use; OA articles are governed by the applicable Creative Commons License

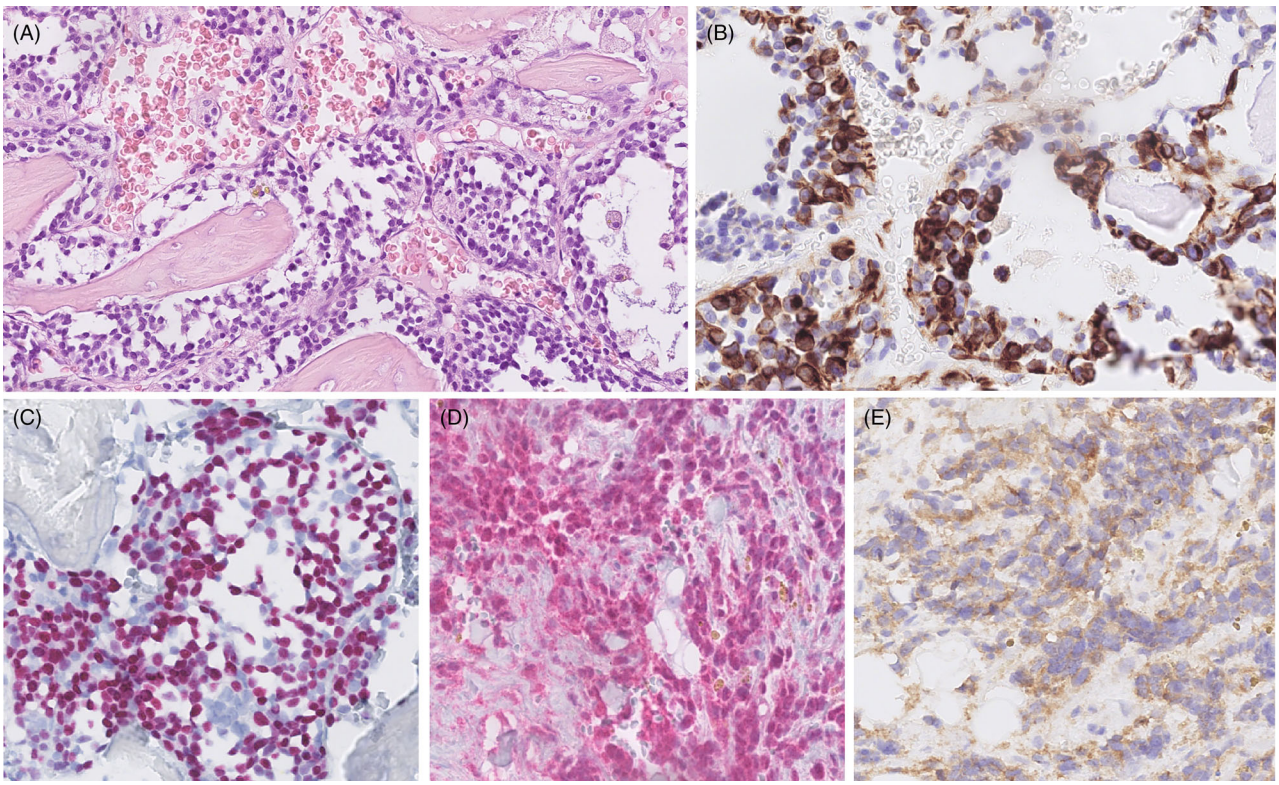


Figure 5. The bone metastasis in case 5 was composed of round cells and lacked intervening stroma (**A**). The tumour cells expressed myogenic markers including desmin (**B**), *MyoD1* (**C**), and myogenin (**D**). *ALK* showed focal cytoplasmic expression (**E**). [Colour figure can be viewed at wileyonlinelibrary.com]

case with concurrent loss of *NF2* and *MTAP* genes.[38] One case carried amplification of the *CDKN2A/B* gene. In one case, amplification of *PDCD1LG2 (PD-L2)*, *JAK2*, and *NFIB* genes was found.[39] In two cases, SNVs were reported, including *CDC73* and *SETD2* in the first case and *AMER1*, *PREX2*, *TFE3*, along with a deletion in the *APC* gene in the second case.[19]

The therapeutic approach included surgery in 26 cases, combined with chemotherapy and/or radiotherapy in 17 cases, which in two cases was followed by tyrosinkinase inhibitors (TRKi). In 20 patients surgery was not performed due to advanced disease and 18 of these patients received chemotherapy and/or radiotherapy and six cases additionally received TRKi. In total, TRKi was administered in eight patients including pazopanib, alectinib, crizotinib, and/or lorlatinib.

Twenty patients developed one or more distant metastases (either at the time of diagnosis or after disease progression) to bones (n = 13), lungs (n = 12), liver (n = 1), and the gastrointestinal tract (n = 1). Of note, lymph node metastases occurred in 11 cases and were usually present at the time of diagnosis.

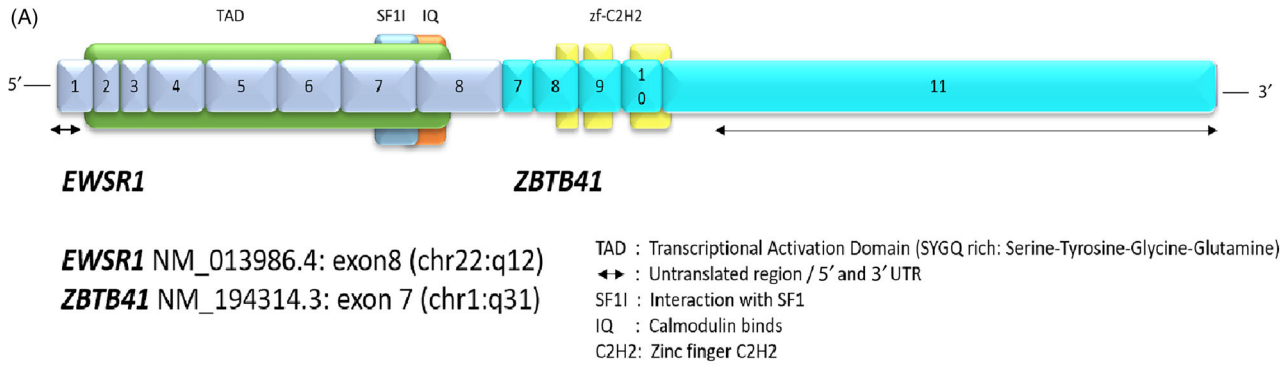
Follow-up was available for 50 cases (75.8%), with an average follow-up period of 15.7 months (mean 11 months, range 0–108 months). Seven patients (14%) were alive without evidence of disease, with an average of follow-up of 32.4 months (mean 27.5 months, range 2–108 months). Eighteen patients (36%) were alive with disease after an average 15.6 months of follow-up (mean 9 months, range 0–60 months). Twenty-five patients (50%) died of disease within (on average) 10.9 months (median 9.5 months, range 1–34 months).

One of our cases (not involved in the description above) had hitherto undescribed *EWSR1::ZBTB41* gene fusion, and additional case showed novel *PLOD2::RBM6* gene fusion. The same case developed *PTPRT c.795C > A p.(Tyr265Ter)* gene mutation and amplification of the *PDGFRA* gene.

STATISTICAL ANALYSIS

Various clinical parameters were statistically evaluated as potential predictors of patient OS. The variables included: sex, age, *EWSR1*, *FUS*, *ALK*, and *CDKN2A/B* genetic events, influence of surgery,

13652559, 2024, 5, Downloaded from https://onlinelibrary.wiley.com/doi/10.1111/his.15121 by Ukraine - Cochrane, Wiley Online Library on [17/12/2024]. See the Terms and Conditions (https://onlinelibrary.wiley.com/terms-and-conditions) on Wiley Online Library for rules of use; OA articles are governed by the applicable Creative Commons License



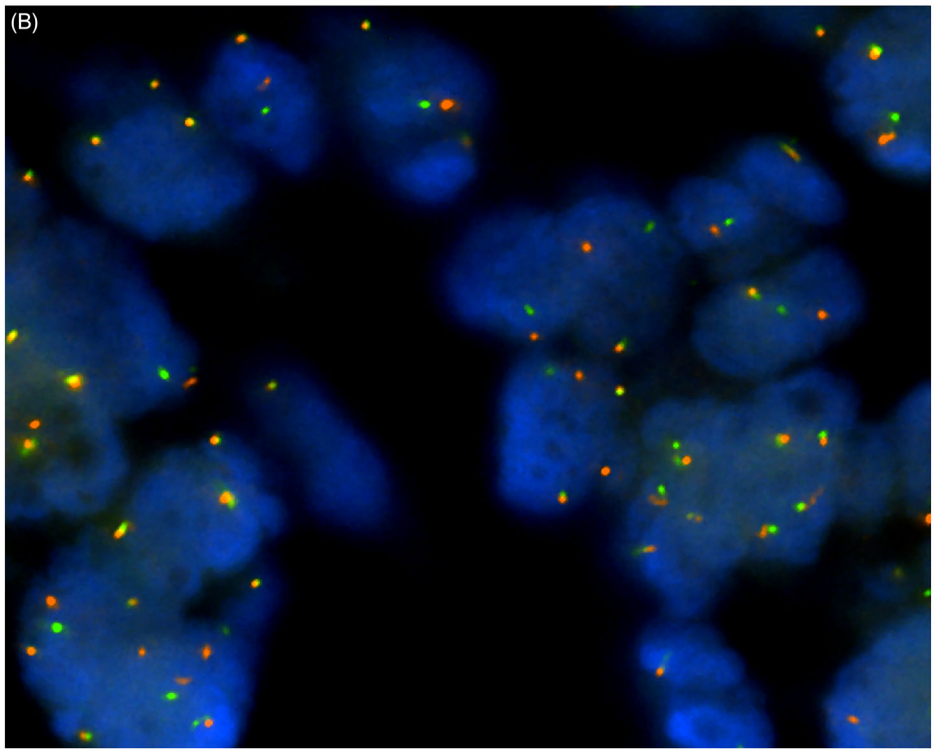


Figure 6. The fusion joining the exon 8 of *EWSR1* with exon 7 of *ZBTB41* is illustrated and protein domains are depicted (**A**). The FISH analysis using the *ZBTB41* probe showed yellow signal (normal) and separated orange and green signals indicating a break of *ZBTB41* gene (**B**). [Colour figure can be viewed at wileyonlinelibrary.com]

radiotherapy (RT), chemotherapy (CHT), and/or biological treatment. All prognostically relevant parameters are listed in Table 4.

The OS curve was valid (59% of the data were censored). The OS median was 7 months. The 0.5-1-year OS was 72%, the 1-year OS was 57%, but a 3-year OS dropped to 28% (Figure 8A). Gender did not have any influence on OS ($P = 0.6665$). Age-related OS was statistically significant when divided into quartiles, including <17, 18–24, 25–49, and >50 years of age ($P = 0.0370$; Figure 8B). The OS was dependent on age. Patients between 18 and 24 years of age had the worst prognosis; the 0.5-year OS was 64% and the 1- and 3-year OS was 0% (mean 0.667 years). The strongest cutoff for age-dependent OS was 50 years of age, which showed a borderline statistically insignificant difference ($P = 0.0526$).

The presence of *EWSR1* or *FUS* gene alterations did not influence OS ($P = 0.3321$ and $P = 0.1663$, respectively). The presence of the *ALK* gene mutation or fusion was related to a 2.9 hazard ratio ($P = 0.0069$) and 0.5-year OS for *ALK*-altered cases was 55%, whereas 0.5-year OS in ALK-negative cases

13652559, 2024, 5, Downloaded from https://onlinelibrary.wiley.com/doi/10.1111/his.15121 by Ukraine - Cochrane, Wiley Online Library on [17/12/2024]. See the Terms and Conditions (https://onlinelibrary.wiley.com/terms-and-conditions) on Wiley Online Library for rules of use; OA articles are governed by the applicable Creative Commons License

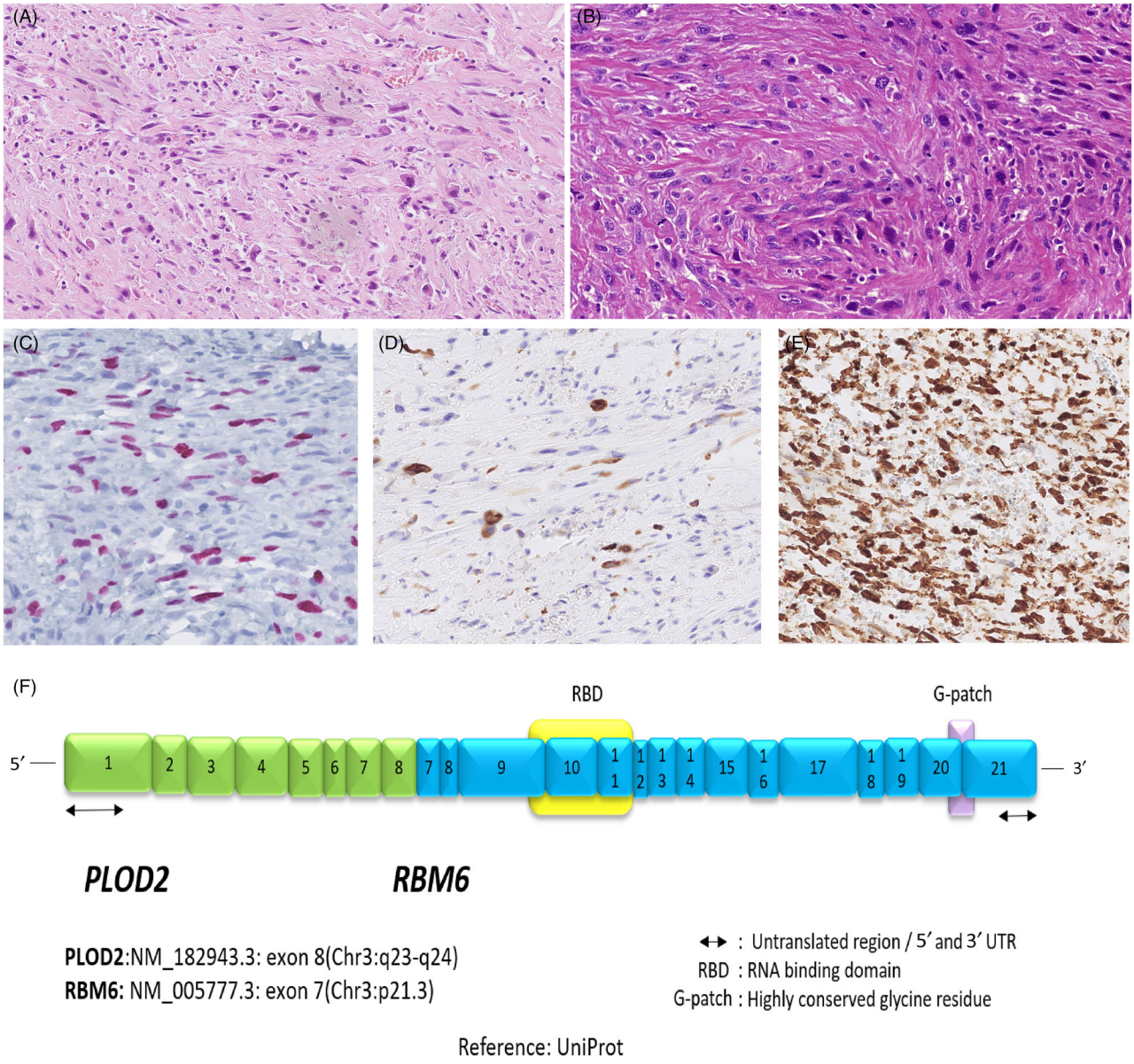


Figure 7. Case 6 was a relatively hypocellular lesion composed of vague fascicles of irregular spindle-shaped cells with intervening hyalinized stroma (**A**). Occasional areas with increased cellularity, higher nuclear pleomorphism, hyperchromatic nuclei, and increased mitotic activity were present (**B**). Tumour cells showed focal expression of *MyoD1* (**C**) and desmin (**D**). SMA was diffusely positive (**E**). The fusion joining of exon 8 of *PLOD2* with exon 7 of *RBM6* is illustrated and protein domains are depicted (**F**). [Colour figure can be viewed at wileyonlinelibrary.com]

was 79% (Figure 9A). Similarly, the presence of a *CDKN2A/2B* alteration was correlated with a worse prognosis, with a 2.9 hazard ratio ($P = 0.0246$) and the 0.5-year OS was 59% for positive and 77% for negative cases (Figure 9B).

Treatment by standard CHT had a negative impact on OS ($P = 0.0410$), with a 4.255 hazard ratio because of worse clinical stage at the time of diagnosis (Figure 9C). There was no significant difference between patients treated by RT, or biological treatment compared to the group of patients treated by other means ($P = 0.1868$ and $P = 0.3245$, respectively). Also, a combination of different treatment modalities radiotherapy + chemotherapy ($P = 0.1224$), or chemotherapy + radiotherapy + biological treatment ($P = 0.3861$) was of no statistical significance (Figure 9D). The Cox regression model showed that the group of patients without

13652559, 2024, 5, Downloaded from https://onlinelibrary.wiley.com/doi/10.1111/his.15121 by Ukraine - Cochrane, Wiley Online Library on [17/12/2024]. See the Terms and Conditions (https://onlinelibrary.wiley.com/terms-and-conditions) on Wiley Online Library for rules of use; OA articles are governed by the applicable Creative Commons License

Table 4. Overall survival of selected prognostically relevant parameters

Parameter	Categories	Number of cases	0.5-year OS (%)	1-year OS (%)	3-year OS (%)	Mean survival (years)	SE
OS	None	66	72	57	28	1.563	0.165
Age (years)	<17	12	90	68	0	1.274	0.147
	18–24	11	64	0	0	0.667	0.121
	25–49	27	59	38	29	1.149	0.182
	>50	14	82	82	45	2.239	0.344
	All <49	50	68	34	22	1.130	0.121
ALK	Positive	15	55	23	0	0.845	0.164
	Negative	51	79	66	35	1.785	0.194
CDKN2A/2B	Positive	15	59	34	13	0.772	0.111
	Negative	52	77	66	32	1.775	0.195

OS, Overall survival.

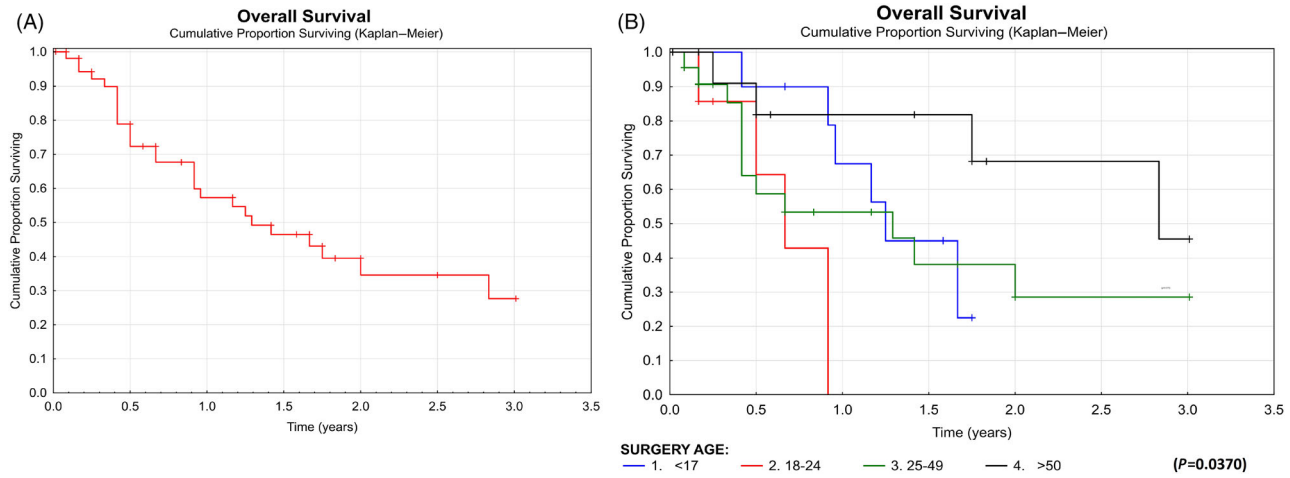


Figure 8. Overall survival (OS) of TFCP2 SS-RMS by Kaplan–Meier univariate analysis (**A**). OS by Kaplan–Meier multivariate analysis, which emphasized that OS was related to age and the worst survival was in category of patients between 18 and 24 years ($P = 0.0370$) (**B**). [Colour figure can be viewed at wileyonlinelibrary.com]

(neo)adjuvant treatment had a borderline statistically insignificant difference of better OS compared to the group of patients treated with combination therapy ($P = 0.0643$). That was related to advanced stage (which was available in less than half of the cases) and disease dissemination in patients who were treated by (neo)adjuvant modalities and were naturally of poor clinical status.

Finally, multivariate the Cox regression hazard model was performed (included variables were age, sex, presence of *EWSR1*, *FUS*, and *ALK*-gene alterations, *CDKN2A/2B* alteration). The only statistically significant variable was the presence of *ALK*-gene alteration ($P = 0.0151$), with a hazard ratio of 2.796.

Disease-free survival was impossible to calculate, as most patients did not have a complete tumour resection and therefore had no tumour-free period.

Discussion

SS-RMS represents a genetically heterogeneous group of RMS, with three molecular variants currently recognized. Spindle-cell RMS with *VGLL2/NCOA1/CITED2* gene rearrangements[7,8] affects newborns or infants,

13652559, 2024, 5, Downloaded from https://onlinelibrary.wiley.com/doi/10.1111/his.15121 by Ukraine - Cochrane, Wiley Online Library on [17/12/2024]. See the Terms and Conditions (https://onlinelibrary.wiley.com/terms-and-conditions) on Wiley Online Library for rules of use; OA articles are governed by the applicable Creative Commons License

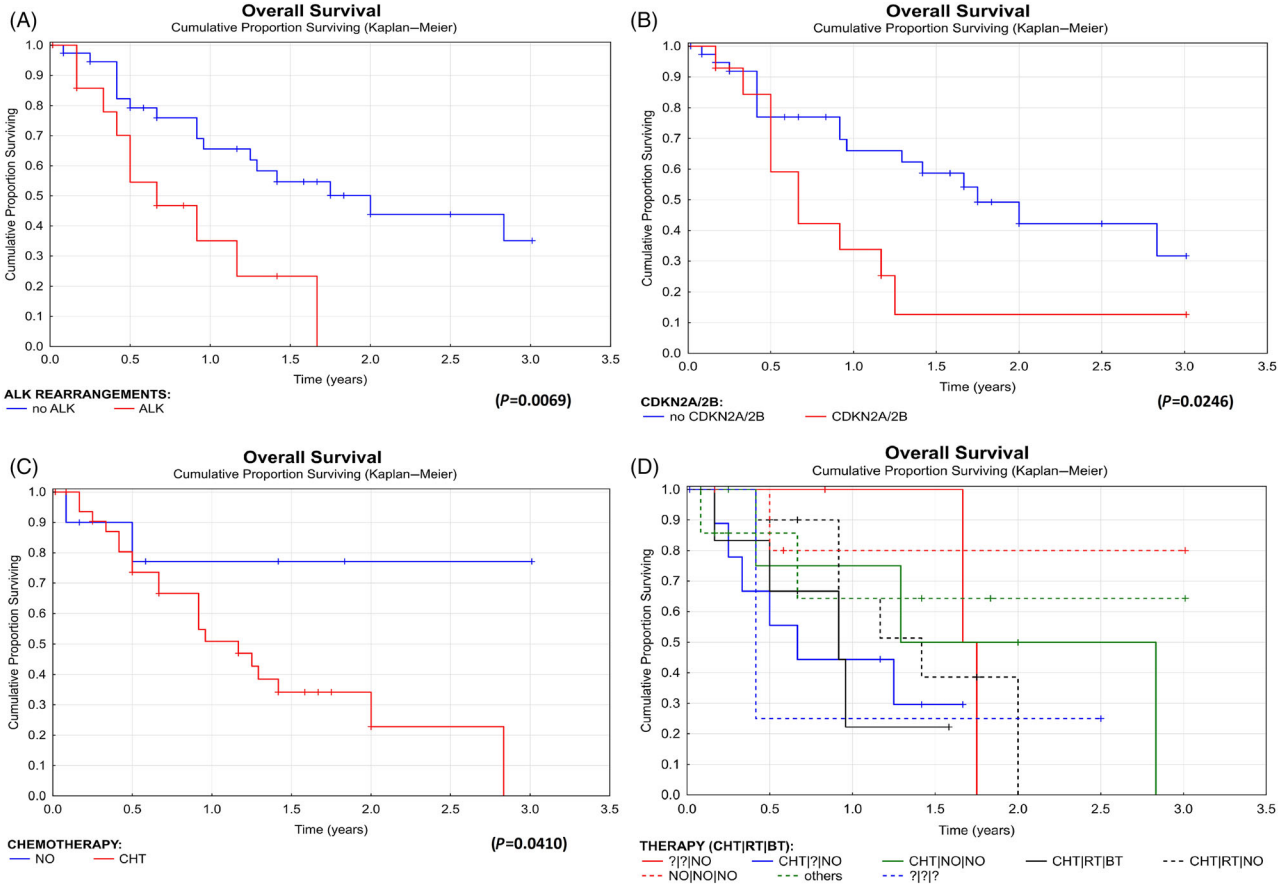


Figure 9. Overall survival (OS) of TFCP2 SS-RMS by Kaplan–Meier univariate analysis, which emphasized that *OS* was dependent on the presence of the *ALK* gene mutation or fusion, which was associated with a 2.9 hazard ratio ($P = 0.0069$) and a 0.5-year *OS* for *ALK*- rearranged cases was 55% (**A**). Similarly, the *OS* was dependent on the presence of *CDKN2A/2B* alterations with 59% ($P = 0.0246$) 0.5-year OS (**B**). A negative correlation was also present in patients treated by chemotherapy because of their worse clinical stage at the time of diagnosis ($P = 0.0410$) (**C**). OS by Kaplan–Meier univariate analysis for all treatment modalities and their combinations (**D**). [Colour figure can be viewed at wileyonlinelibrary.com]

usually has a good prognosis without a propensity for metastatic spread, and aggressive multimodal therapy may thus not be required.[8] The characteristic molecular genetic events consist of *VGLL2::CITED3*, *VGLL2::NCOA2*, *TEAD1::NCOA2*, or *SRF::NCOA2* gene fusions.[7,8] Only four reported cases developed metastasis, of which three showed high-grade morphology at relapse with genomic instability and alterations of different genes (in particular *TP53*, *CDKN2A/B*, and *FGFR4*).[42] Recently, Agaimy *et al.* described a series of six cases with novel *VGLL3* rearrangements with *TCF12*, *EP300*, and *PPARGC1A* being the fusion partners. Clinically, while these tumours occurred in adults, they again showed H&N predilection and appeared to follow an indolent course.[17]

The second subtype of SS-RMS is *MYOD1*-mutant RMS.[8–12] In contrast to a previous group, this tumour type is typically diagnosed in older children and young adults, represents an aggressive variant, and usually shows sclerosing morphology. Genetically, homozygous or heterozygous *MYOD1* (Leu122Arg) mutations are present,[43] with comutations in the PI3K-AKT pathway (most frequently the *PIK3CA* gene) being present in up to 33% of cases.[8,12] Additional coexistent mutations may be in the RAS pathway, including *NRAS*, *HRAS*, or *FGFR4* gene mutations.[8] The presence of concomitant mutations probably does not change the prognosis, as all cases have a similarly aggressive clinical course, usually paired with resistance to multimodal therapy.[12]

The recently described SS-RMS with *TFCP2* rearrangements again represent aggressive tumours resistant to multimodal therapy, which leads to their overall poor prognosis.[13–15] The literature (including our three cases) contained data on 68 cases of *TFCP2*-rearranged SS-RMS.

13652559, 2024, 5, Downloaded from https://onlinelibrary.wiley.com/doi/10.1111/his.15121 by Ukraine - Cochrane, Wiley Online Library on [17/12/2024]. See the Terms and Conditions (https://onlinelibrary.wiley.com/terms-and-conditions) on Wiley Online Library for rules of use; OA articles are governed by the applicable Creative Commons License

TFCP2 gene (transcription factor cellular promoter 2), also known as *LSF*, is a protooncogene involved in DNA synthesis and cell survival and works as an antiapoptotic factor.[44] *TFCP2* has been reported to be involved in hepatocellular, pancreatic, renal, thyroid, oral, breast, cervical, and colorectal cancer.[45,46]

Hemizygous deletion or amplification of the *ALK* gene was reported in 11 and 2 SS-RMS cases, respectively. An additional two reported cases carried double or triple *ALK* gene fusions, namely, one case with *FUS::TFCP2* and *TIMP3::ALK* gene fusion[39] and a second case with *FUS::TFCP2* and dual *VAX2::ALK (VAX2ex2::ALKex2* and *VAX2intron2::ALKex2)* gene fusion.

ALK inhibitors represent an effective treatment for advanced *ALK*-fused tumours, particularly in non-small-cell lung cancer, but the experience with ALK inhibitors in sarcomas is more limited, with only a few tumour types targeted by this treatment, including inflammatory myofibroblastic tumour.[39,47–50] Overall, nine *TFCP2*-rearranged RMS patients were treated by TRKi (crizotinib, alectinib, lorlatinib, and/or pazopanib), either alone or in combination with chemotherapy and/or radiotherapy. Five patients died of the disease after 7.7 months of an average follow-up period, two patients were alive with disease 8 and 19 months after the diagnosis, and one patient was alive without evidence of disease at 17 months after diagnosis (one case was lost for follow-up). From this group, five of nine patients showed *ALK*-alteration (three cases carried *ALK*-deletion and two cases *ALK*-fusion).

Anecdotal cases have been reported in which the combination of ALK inhibitors and radiotherapy resulted in disease stabilization.[29,36] This therapeutical option appears to be effective in primary *TFCP2*-rearranged RMS where *ALK* gene alteration has been identified. However, recurrences or metastases of these tumours usually lacked any *ALK*-gene alterations.[15,26,29,33,36,39,41]

Six patients were treated with a combination of CHT and/or RT and biological treatment (without surgery), in particular ALK inhibitors (including alectinib, crizotinib, and/or lorlatinib) or vascular endothelial growth factor inhibitors (pazopanib). These were used either alone or in combination in six and three cases, respectively. Except for two patients who are alive with the disease, all others progressed despite treatment and died of the disease.[39]

Thirteen *TFCP2*-rearranged SS-RMS harboured homozygous deletion of *CDKN2A* or *CDKN2B* ($n = 12$) or had amplification of *CDKN2A* and *CDKN2B* genes ($n = 1$),[14,15,36,38–40] but none showed concurrent inactivation of *TP53*, associated with a worse outcome in other RMS types, mainly in pleomorphic RMS.[51] *CDKN2A/B* genes might be another potential target, but none of the cases reported in the literature were treated by CDK4/6 inhibitors that could be efficient drugs in tumours with a high CDK4 level.[52]

A novel *EWSR1ex8::ZBTB4ex7* gene fusion was detected in case 4. The tumour showed monotonous round/ovoid cell morphology and was diffusely positive for rhabdomyoblastic markers (MyoD1, desmin, and myogenin), was negative for pancytokeratins and showed patchy positivity for ALK. The *ZBTB4* (zinc finger and BTB domain containing 4) is a transcriptional repressor gene that was described across different human malignancies including breast, ovary, prostate, or neuroblastoma.[53,54] It is involved in the activation of the p53 gene by regulation of the activity of CDKN1A. Downregulation of *ZBTB4* inhibits apoptosis and increases tumour cell growth. Yu *et al.* proposed a theory that *in vitro* restoration of the inactivated *ZBTB4* gene in Ewing sarcoma cells reduces their survival via decreasing Survivin expression.[55] This theory supported the study of drug-induced upregulation of the *ZBTB4* gene in prostate cancer by drug targeting of miRNA.[56]

In case 5, we found a novel *PLOD2 exon2::RBM6exon7* gene fusion that has never been described so far in any human malignancy. *RBM6*, RNA Binding Motif protein 6, is a nuclear protein expressed across different human tissues but mainly in the haematopoietic tissue where it participates in the development of T-cells and granulocytes and in nonhematogenic structures. The highest expression is in the heart, pancreas, and skeletal muscle.[57] *RBM6* belongs to the family of tumour-suppressor genes and is responsible for regulation of homologous recombination of double-strand breaks. RBM6-deficient tumours are sensitive to ataxia-telangiectasia mutated (ATM) and poly ADP-ribose polymerase (PARP) inhibitors and may exhibit vulnerability to cisplatin treatment.[58] PLOD2, procollagen-lysine, 2-oxoglutarate 5-dioxygenase 2, is an enzyme that is responsible for increasing cytoplasmic succinate, thereby activating the epithelial-mesenchymal transition, an ability responsible for metastatic spread and drug resistance.[59] The same case harboured a *PTPRT c.795C>A p.(Tyr265Ter)* gene mutation as well as amplification of the *PDGFRA* gene.

In conclusion, *TFCP2*-rearranged SS-RMS is a rare and very aggressive subtype of RMS. The frequent pancytokeratin expression represents a diagnostic challenge. Therefore, the awareness of its salient

13652559, 2024, 5, Downloaded from https://onlinelibrary.wiley.com/doi/10.1111/his.15121 by Ukraine - Cochrane, Wiley Online Library on [17/12/2024]. See the Terms and Conditions (https://onlinelibrary.wiley.com/terms-and-conditions) on Wiley Online Library for rules of use; OA articles are governed by the applicable Creative Commons License

clinicopathological features, namely, its common occurrence in craniofacial bones of young adults, epithelioid, and spindled morphology coupled with the expression of rhabdomyoblastic markers and frequent ALK positivity are clues to the correct diagnosis. The disease has a rapid clinical course, with poor prognosis (3-year overall survival rate 28%). *CDKN2A* or *ALK* alterations, the use of standard chemotherapy, and age at presentation of 18–24 years are negatively correlated with overall survival.

Author contributions

MB, MM, SK, MM, and MŠ: conception and design of the work, acquisition, analysis, and interpretation of data, drafting the article and revising it critically for important intellectual content and scientific integrity. EM, TV, and PG: performance and interpretation of molecular-genetic analysis, revising it critically for important intellectual content, and scientific integrity. OK, ZK, ŠL, AN, LS, and MF: providing the case, reading and revising the article critically for important intellectual content and scientific integrity. All the authors have read and approved the final article.

Funding information

This study was in part supported by study grant SVV 260652 from the Ministry of Education, Czech Republic, the Cooperation Program, research area SURG, and the project National Institute for Cancer Research—NICR (Programme EXCELES, ID project no. LX22NPO5102)—Funded by the European Union —Next Generation EU.

Conflict of interest statement

The authors disclose that they have no significant relationships with, or financial interest in, any commercial companies pertaining to this article.

Data availability statement

Data supporting the findings of this study are available within the article. The complete datasets generated during and/or analysed during the current study are available from the corresponding author upon reasonable request. All data generated or analysed during this study are included in this published article (and its supplementary information files).

© 2023 John Wiley & Sons Ltd.,

References

1. Rekhi B, Gupta C, Chinnaswamy G *et al*. Clinicopathologic features of 300 rhabdomyosarcomas with emphasis upon differential expression of skeletal muscle specific markers in the various subtypes: a single institutional experience. *Ann. Diagn. Pathol.* 2018; **36**; 50–60.
2. Weiel JJ, Kokh D, Charville GW, Longacre TA. PAX7 is a sensitive marker of skeletal muscle differentiation in rhabdomyosarcoma and tumors with Rhabdomyosarcomatous differentiation in the female genital tract. *Int. J. Gynecol. Pathol.* 2022; **41**; 235–243.
3. WHO Classification of Tumours Editorial Board. Soft tissue and bone tumours. In *WHO classification of tumours series*. Vol. **3**. 5th ed. Lyon, France: International Agency for Research on Cancer, 2020. https://publications.iarc.fr/588
4. Agaram NP, Szuhai K. Spindle cell/sclerosing rhabdomyosarcoma. In *WHO classification of Tumours editorial board soft tissue and bone tumors*. 5th ed. Lyon: International Agency for Research on Cancer., vol 3. WHO classification of tumours series, 211–213, 2020. https://publicationsiarcfr/588.
5. Cavazzana AO, Schmidt D, Ninfo V *et al*. Spindle cell rhabdomyosarcoma. A prognostically favorable variant of rhabdomyosarcoma. *Am. J. Surg. Pathol.* 1992; **16**; 229–235.
6. WHO Classification of Tumours Editorial Board. *Soft tissue and bone tumours*. (WHO classification of tumours series, 5th ed, vol. 3). Lyon: International Agency for Research on Cancer, 2020. https://publications.iarc.fr/588.
7. Mosquera JM, Sboner A, Zhang L *et al*. Recurrent NCOA2 gene rearrangements in congenital/infantile spindle cell rhabdomyosarcoma. *Genes Chromosomes Cancer* 2013; **52**; 538–550.
8. Alaggio R, Zhang L, Sung YS *et al*. A molecular study of pediatric spindle and sclerosing rhabdomyosarcoma: identification of novel and recurrent VGLL2-related fusions in infantile cases. *Am. J. Surg. Pathol.* 2016; **40**; 224–235.
9. Szuhai K, de Jong D, Leung WY, Fletcher CDM, Hogendoorn PCW. Transactivating mutation of the MYOD1 gene is a frequent event in adult spindle cell rhabdomyosarcoma. *J. Pathol.* 2014; **232**; 300–307.
10. Kohsaka S, Shukla N, Ameur N *et al*. A recurrent neomorphic mutation in MYOD1 defines a clinically aggressive subset of embryonal rhabdomyosarcoma associated with PI3K-AKT pathway mutations. *Nat. Genet.* 2014; **46**; 595–600.
11. Agaram NP, Chen CL, Zhang L, LaQuaglia MP, Wexler L, Antonescu CR. Recurrent MYOD1 mutations in pediatric and adult sclerosing and spindle cell rhabdomyosarcomas: evidence for a common pathogenesis. *Genes Chromosomes Cancer* 2014; **53**; 779–787.
12. Agaram NP, LaQuaglia MP, Alaggio R *et al*. MYOD1-mutant spindle cell and sclerosing rhabdomyosarcoma: an aggressive subtype irrespective of age. A reappraisal for molecular classification and risk stratification. *Mod. Pathol.* 2019; **32**; 27–36.
13. Watson S, Perrin V, Guillemot D *et al*. Transcriptomic definition of molecular subgroups of small round cell sarcomas. *J. Pathol.* 2018; **245**; 29–40.
14. Dashti NK, Wehrs RN, Thomas BC *et al*. Spindle cell rhabdomyosarcoma of bone with FUS-TFCP2 fusion: confirmation of a very recently described rhabdomyosarcoma subtype. *Histopathology* 2018; **73**; 514–520.
15. Le Loarer F, Cleven AHG, Bouvier C *et al*. A subset of epithelioid and spindle cell rhabdomyosarcomas is associated with TFCP2 fusions and common ALK upregulation. *Mod. Pathol.* 2020; **33**; 404–419.

13652559, 2024, 5, Downloaded from https://onlinelibrary.wiley.com/doi/10.1111/his.15121 by Ukraine - Cochrane, Wiley Online Library on [17/12/2024]. See the Terms and Conditions (https://onlinelibrary.wiley.com/terms-and-conditions) on Wiley Online Library for rules of use; OA articles are governed by the applicable Creative Commons License

16. Han R, Dermawan JK, Demicco EG *et al.* ZFP64::NCOA3 gene fusion defines a novel subset of spindle cell rhabdomyosarcoma. *Genes Chromosomes Cancer* 2022; **61**; 645–652.
17. Agaimy A, Dermawan JK, Leong I *et al.* Recurrent VGLL3 fusions define a distinctive subset of spindle cell rhabdomyosarcoma with an indolent clinical course and striking predilection for the head and neck. *Genes Chromosomes Cancer* 2022; **61**; 701–709.
18. Yoshida KI, Kukita Y, Nakamura H, Nakai S, Honma K, Yagi T. A case of spindle cell rhabdomyosarcoma with an EP300::VGLL3 fusion. *Genes Chromosomes Cancer* 2023; **62**; 184–186.
19. Dehner CA, Broski SM, Meis JM *et al.* Fusion-driven spindle cell rhabdomyosarcomas of bone and soft tissue: a clinicopathologic and molecular genetic study of 25 cases. *Mod. Pathol.* 2023; **36**; 100271. https://doi.org/10.1016/j.modpat.2023.100271
20. Skalova A, Ptakova N, Santana T *et al.* NCOA4-RET and TRIM27-RET are characteristic gene fusions in salivary intraductal carcinoma, including invasive and metastatic tumors: is "Intraductal" correct? *Am. J. Surg. Pathol.* 2019; **43**; 1303–1313.
21. https://www.illumina.com/content/dam/illumina-marketing/documents/products/gene_lists/gene_list_trusight_oncology_500.xlsx.
22. https://emea.support.illumina.com/content/dam/illumina-support/documents/downloads/productfiles/trusight/trusight-rna-pan-cancer-target-regions-gtf.zip.
23. Skalova A, Baneckova M, Laco J *et al.* Sclerosing polycystic adenoma of salivary glands: a novel neoplasm characterized by PI3K-AKT pathway alterations-new insights into a challenging entity. *Am. J. Surg. Pathol.* 2022; **46**; 268–280.
24. Skalova A, Agaimy A, Vanecek T *et al.* Molecular profiling of clear cell myoepithelial carcinoma of salivary glands with EWSR1 rearrangement identifies frequent PLAG1 gene fusions but no EWSR1 fusion transcripts. *Am. J. Surg. Pathol.* 2021; **45**; 1–13.
25. Agaram NP, Zhang L, Sung YS *et al.* Expanding the spectrum of intraosseous rhabdomyosarcoma: correlation between 2 distinct gene fusions and phenotype. *Am. J. Surg. Pathol.* 2019; **43**; 695–702.
26. Lewin J, Desai J, Smith K, Luen S, Wong D. Lack of clinical activity with crizotinib in a patient with FUS rearranged rhabdomyosarcoma with ALK protein overexpression. *Pathology* 2019; **51**; 655–657.
27. Tagami Y, Sugita S, Kubo T *et al.* Spindle cell rhabdomyosarcoma in a lumbar vertebra with FUS-TFCP2 fusion. *Pathol. Res. Pract.* 2019; **215**; 152399.
28. Chrisinger JSA, Wehrli B, Dickson BC *et al.* Epithelioid and spindle cell rhabdomyosarcoma with FUS-TFCP2 or EWSR1-TFCP2 fusion: report of two cases. *Virchows Arch.* 2020; **477**; 725–732.
29. Brunac AC, Laprie A, Castex MP *et al.* The combination of radiotherapy and ALK inhibitors is effective in the treatment of intraosseous rhabdomyosarcoma with FUS-TFCP2 fusion transcript. *Pediatr. Blood Cancer* 2020; **67**; e28185.
30. Koutlas IG, Olson DR, Rawwas J. FET(EWSR1)-TFCP2 rhabdomyosarcoma: an additional example of this aggressive variant with predilection for the gnathic bones. *Head Neck Pathol.* 2021; **15**; 374–380.
31. Xu B, Suurmeijer AJH, Agaram NP, Zhang L, Antonescu CR. Head and neck rhabdomyosarcoma with TFCP2 fusions and ALK overexpression: a clinicopathological and molecular analysis of 11 cases. *Histopathology* 2021; **79**; 347–357.
32. Ochsner AR, Foss RD. Epithelioid and spindle cell rhabdomyosarcoma of the oral mucosa with FUS rearrangement. *Head Neck Pathol.* 2022; **16**; 823–827.
33. Panferova A, Sinichenkova KY, Abu Jabal M *et al.* EWSR1-TFCP2 in an adolescent represents an extremely rare and aggressive form of intraosseous spindle cell rhabdomyosarcomas. *Cold Spring Harb. Mol. Case Stud.* 2022; **8**; 8.
34. Silva Cunha JL, Cavalcante IL, da Silva Barros CC *et al.* Intraosseous rhabdomyosarcoma of the maxilla with TFCP2 fusion: a rare aggressive subtype with predilection for the gnathic bones. *Oral Oncol.* 2022; **130**; 105876.
35. Ishiyama T, Kato I, Ito J *et al.* Rhabdomyosarcoma with FUS::TFCP2 fusion in the scalp: a rare case report depicting round and spindle cell morphology. *Int. J. Surg. Pathol.* 2023; **31**; 805–812.
36. Valerio E, Furtado Costa JL, Perez Fraile NM *et al.* Intraosseous spindle cell/epithelioid rhabdomyosarcoma with TFCP2 rearrangement: a recent recognized subtype with partial response to Alectinib. *Int. J. Surg. Pathol.* 2023; **31**; 861–865.
37. Gallagher KPD, Roza A, Tager E *et al.* Rhabdomyosarcoma with TFCP2 rearrangement or typical co-expression of AE1/AE3 and ALK: report of three new cases in the head and neck region and literature review. *Head Neck Pathol.* 2022; **17**; 546–561.
38. Ma Y, Feng J, Ding D, Zhao J, Tian F. TFCP2-rearranged epithelioid and spindle cell rhabdomyosarcoma in the bladder: a rare case in an 8-year-old female child. *Pediatr. Blood Cancer* 2023; **70**; e29935.
39. Duan FL, Yang H, Gong X *et al.* Clinicopathological features of rhabdomyosarcoma with novel FET::TFCP2 and TIMP3::ALK fusion: report of two cases and literature review. *Histopathology* 2023; **82**; 478–484.
40. Carrillo-Ng H, Liang Y, Chang S *et al.* Complete mimicry: rhabdomyosarcoma with FUS::TFCP2 fusion masquerading as carcinoma-diagnostic challenge and report of two cases. *Genes Chromosomes Cancer* 2023; **62**; 430–436.
41. Wong DD, van Vliet C, Gaman A, Giardina T, Amanuel B. Rhabdomyosarcoma with FUS re-arrangement: additional case in support of a novel subtype. *Pathology* 2019; **51**; 116–120.
42. Cyrta J, Gauthier A, Karanian M *et al.* Infantile rhabdomyosarcomas with VGLL2 rearrangement are not always an indolent disease: a study of 4 aggressive cases with clinical, pathologic, molecular, and radiologic findings. *Am. J. Surg. Pathol.* 2021; **45**; 854–867.
43. Van Antwerp ME, Chen DG, Chang C *et al.* A point mutation in the MyoD basic domain imparts c-Myc-like properties. *Proc. Natl. Acad. Sci. U. S. A.* 1992; **89**; 9010–9014.
44. Yoo BK, Emdad L, Gredler R *et al.* Transcription factor late SV40 factor (LSF) functions as an oncogene in hepatocellular carcinoma. *Proc. Natl. Acad. Sci. U. S. A.* 2010; **107**; 8357–8362.
45. Kotarba G, Krzywinska E, Grabowska AI, Taracha A, Wilanowski T. TFCP2/TFCP2L1/UBP1 transcription factors in cancer. *Cancer Lett.* 2018; **420**; 72–79.
46. Taracha A, Kotarba G, Wilanowski T. Neglected functions of TFCP2/TFCP2L1/UBP1 transcription factors may offer valuable insights into their mechanisms of action. *Int. J. Mol. Sci.* 2018; **19**; 2852. https://doi.org/10.3390/ijms19102852
47. Sun Y, Nowak KA, Zaorsky NG *et al.* ALK inhibitor PF02341066 (crizotinib) increases sensitivity to radiation in non-small cell lung cancer expressing EML4-ALK. *Mol. Cancer Ther.* 2013; **12**; 696–704.

13652559, 2024, 5, Downloaded from https://onlinelibrary.wiley.com/doi/10.1111/his.15121 by Ukraine - Cochrane, Wiley Online Library on [17/12/2024]. See the Terms and Conditions (https://onlinelibrary.wiley.com/terms-and-conditions) on Wiley Online Library for rules of use; OA articles are governed by the applicable Creative Commons License

48. Dai Y, Wei Q, Schwager C *et al.* Synergistic effects of crizotinib and radiotherapy in experimental EML4-ALK fusion positive lung cancer. *Radiother. Oncol.* 2015; **114**; 173–181.
49. Mahajan P, Casanova M, Ferrari A, Fordham A, Trahair T, Venkatramani R. Inflammatory myofibroblastic tumor: molecular landscape, targeted therapeutics, and remaining challenges. *Curr. Probl. Cancer* 2021; **45**; 100768.
50. Theilen TM, Soerensen J, Bochennek K *et al.* Crizotinib in ALK(+) inflammatory myofibroblastic tumors-current experience and future perspectives. *Pediatr. Blood Cancer* 2018; **65**. https://doi.org/10.1002/pbc.26920
51. Chelsky ZL, Paulson VA, Chen EY. Molecular analysis of 10 pleomorphic rhabdomyosarcomas reveals potential prognostic markers and druggable targets. *Genes Chromosomes Cancer* 2022; **61**; 138–147.
52. Perez M, Munoz-Galvan S, Jimenez-Garcia MP *et al.* Efficacy of CDK4 inhibition against sarcomas depends on their levels of CDK4 and p16ink4 mRNA. *Oncotarget* 2015; **6**; 40557–40574.
53. Weber A, Marquardt J, Elzi D *et al.* Zbtb4 represses transcription of P21CIP1 and controls the cellular response to p53 activation. *EMBO J.* 2008; **27**; 1563–1574.
54. Roussel-Gervais A, Naciri I, Kirsh O *et al.* Loss of the methyl-CpG-binding protein ZBTB4 alters mitotic checkpoint, increases aneuploidy, and promotes tumorigenesis. *Cancer Res.* 2017; **77**; 62–73.
55. Yu Y, Shang R, Chen Y *et al.* Tumor suppressive ZBTB4 inhibits cell growth by regulating cell cycle progression and apoptosis in Ewing sarcoma. *Biomed. Pharmacother.* 2018; **100**; 108–115.
56. Kim K, Chadalapaka G, Pathi SS *et al.* Induction of the transcriptional repressor ZBTB4 in prostate cancer cells by drug-induced targeting of microRNA-17-92/106b-25 clusters. *Mol. Cancer Ther.* 2012; **11**; 1852–1862.
57. Sutherland LC, Rintala-Maki ND, White RD, Morin CD. RNA binding motif (RBM) proteins: a novel family of apoptosis modulators? *J. Cell. Biochem.* 2005; **94**; 5–24.
58. Machour FE, Abu-Zhayia ER, Awwad SW *et al.* RBM6 splicing factor promotes homologous recombination repair of double-strand breaks and modulates sensitivity to chemotherapeutic drugs. *Nucleic Acids Res.* 2021; **49**; 11708–11727.
59. Tong Y, Qi Y, Xiong G *et al.* The PLOD2/succinate axis regulates the epithelial-mesenchymal plasticity and cancer cell stemness. *Proc. Natl. Acad. Sci. U. S. A.* 2023; **120**; e2214942120.

Supporting Information

Additional Supporting Information may be found in the online version of this article:

File S1.

File S2.

13652559, 2024, 5, Downloaded from https://onlinelibrary.wiley.com/doi/10.1111/his.15121 by Ukraine - Cochrane, Wiley Online Library on [17/12/2024]. See the Terms and Conditions (https://onlinelibrary.wiley.com/terms-and-conditions) on Wiley Online Library for rules of use; OA articles are governed by the applicable Creative Commons License